

# *TET2* mutational status affects myelodysplastic syndrome evolution to chronic myelomonocytic leukemia

According to the 4<sup>th</sup> iteration of the World Health Organization (WHO) classification that came out in 2017, a diagnosis of chronic myelomonocytic leukemia (CMML) still required a persistent absolute ( $\geq 1 \times 10^9/L$ ) and relative ( $\geq 10\%$  of white blood cell [WBC] count) monocytosis. Nevertheless, several reports suggested that up to 30% of myelodysplastic syndrome (MDS) evolved into genuine CMML,<sup>1</sup> raising for many years the question of a “pre-CMML” state.<sup>2</sup> An oligo-monocytic CMML entity was subsequently described in patients displaying a relative monocytosis with an absolute monocyte count between  $0.5 \times 10^9/L$  and  $1 \times 10^9/L$ ,<sup>3,4</sup> providing a rationale to revise CMML diagnosis criteria in the recent 5<sup>th</sup> edition of the WHO classification that considers a relative monocytosis  $\geq 10\%$  of WBC and an absolute monocyte count  $\geq 0.5 \times 10^9/L$ .<sup>5</sup> An increased fraction of circulating classical monocytes (cMO, defined by flow cytometry as  $CD14^{++}CD16^{-}$  fraction)  $\geq 94\%$ , which was shown to distinguish CMML from reactive monocytosis,<sup>1,6</sup> was included as a supportive criterion for CMML diagnosis. Notwithstanding these new diagnosis criteria, MDS with bone marrow (BM) monocyte infiltration could represent another group of pre-CMML. The present longitudinal study aims at identifying robust predictors of MDS evolution to “overt” CMML.

Between 2018 and 2020, flow cytometry analysis of monocyte subset partition was performed in 44 patients with non-treated MDS and were included in a learning cohort together with 22 CMML patients (Table 1). In a control group of 19 patients with established, non-treated CMML according to the 2017 WHO classification, flow cytometry analysis of monocyte subsets mostly showed a relative accumulation of cMO  $\geq 94\%$  of total circulating monocytes.<sup>7</sup> The same flow analysis in patients with an MDS diagnosis showed an increase in the fraction of cMO  $\geq 94\%$  in 18 of 44 (41%) patients, a proportion consistent with a previous report.<sup>1</sup> These cases were defined as “CMML-like MDS”, while MDS cases without an increase in the fraction of cMO  $\geq 94\%$  were designated as “other MDS” (n=26) (Table 1; Figure 1A, B).

Patients with a CMML-like MDS were older than other MDS patients ( $P=0.03$ , unpaired *t* test with Welch’s correction). They showed a significantly higher monocyte percentage in their peripheral blood (PB) ( $13.3 \pm 1.5\%$ ) and BM ( $7 \pm 1\%$ ) as compared with other MDS patients (PB:  $8.8 \pm 1.1\%$ ,  $P=0.0226$ ; BM:  $3 \pm 0.2\%$ ,  $P=0.0098$ ; unpaired *t* test with Welch’s correction) while the absolute monocyte count (AMC) and the Revised International Prognostic

Scoring System (R-IPSS) did not differ significantly between the two groups (Figure 1A; Table 1).

Granulocyte-macrophage colony-stimulating factor (GM-CSF) hypersensitivity was previously identified in approximately 90% of CMML patients.<sup>8</sup> In a standard clonogenic assay supplemented with stem cell factor (SCF), erythropoietin (EPO), interleukin 3 (IL-3), and GM-CSF, we observed a higher proportion of colony-forming unit granulocyte-macrophage (CFU-GM) as compared with burst-forming unit-erythroid (BFU-E) cells in CMML ( $78.9 \pm 5.9\%$ ;  $P=0.0009$ ; Mann-Whitney test), CMML-like MDS ( $71.2 \pm 7.5\%$ ;  $P=0.0006$ , Mann-Whitney test) and in other MDS ( $63.7 \pm 7.2\%$ ;  $P=0.0159$ , Mann-Whitney test) (Figure 1C) showing a granulomonocytic differentiation bias. Without GM-CSF, growth factor-independent colony formation was barely detectable in MDS samples, with or without abnormal partition of monocyte subsets. Nevertheless, at low concentrations of GM-CSF, we detected an increased sensitivity of CMML-like MDS progenitor samples to GM-CSF as compared with those from other MDS, at both 0.1 ng/mL ( $P=0.048$ , Mann-Whitney test) and 1 ng/mL ( $P=0.0025$ ; Mann-Whitney test) of GM-CSF (Figure 1D).

The mutational profile was analyzed at diagnosis or during follow-up by next-generation sequencing (NGS) using a targeted panel of 38 genes recurrently mutated in myeloid malignancies as previously described.<sup>9</sup> The mean number of mutations per sample in CMML-like MDS patients ( $3.5 \pm 0.2$ ) was the same as that of CMML patients ( $3.5 \pm 0.3$ ) and significantly higher than that of other MDS patients ( $1.7 \pm 0.3$ ;  $P \leq 0.0001$ , unpaired *t* test with Welch’s correction). In the learning cohort, *TET2* was the most frequently mutated gene in the three groups of patients, with a similar proportion of patients carrying at least one *TET2* mutation in CMML (68.2%) and CMML-like MDS (66.7%) ( $P=0.92$ ,  $\chi^2$  test) while this proportion was lower in other MDS (34.6%;  $P=0.036$ ,  $\chi^2$  test) (Figure 1E).

Sixty-eight *TET2* mutations were identified in the learning cohort, including 52 (76.5%) truncating mutations, 14 (20.6%) missense mutations and two splice site mutations (2.9%). Truncating mutations were widely spread on the entire protein, while missense mutations were only located in the active domain of *TET2*: two in the Cys-N domain, two in the Cys-R domain, two in the low complexity insert, and eight in the double-stranded  $\beta$ -helix domain (DSBH) domain (Figure 2A). Among patients carrying *TET2* mutations, multiple *TET2* mutations were much more frequent among CMML (14/15, 93.3%) and CMML-like MDS

**Table 1.** Clinical and biological characteristics of the learning cohort.

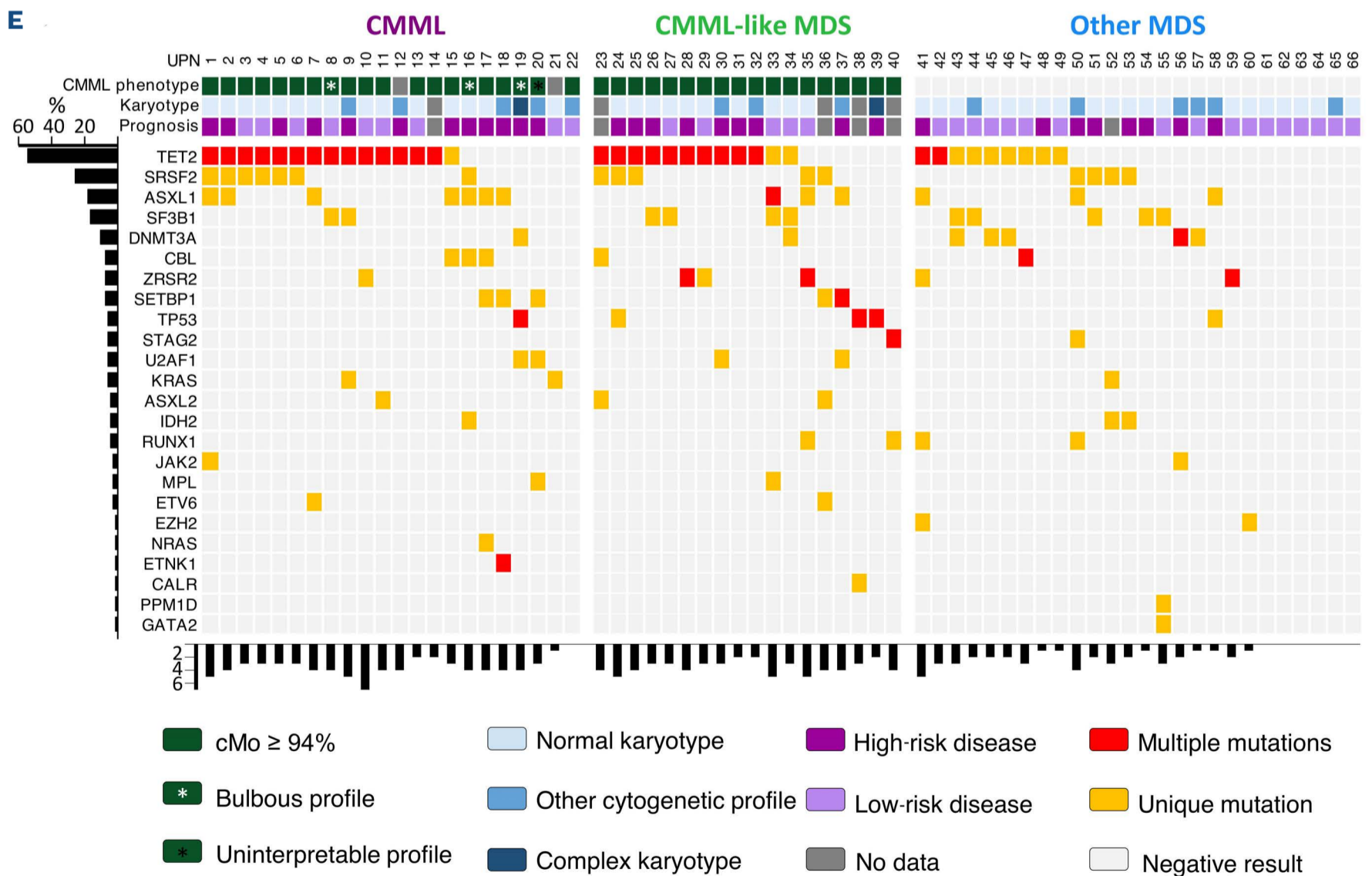
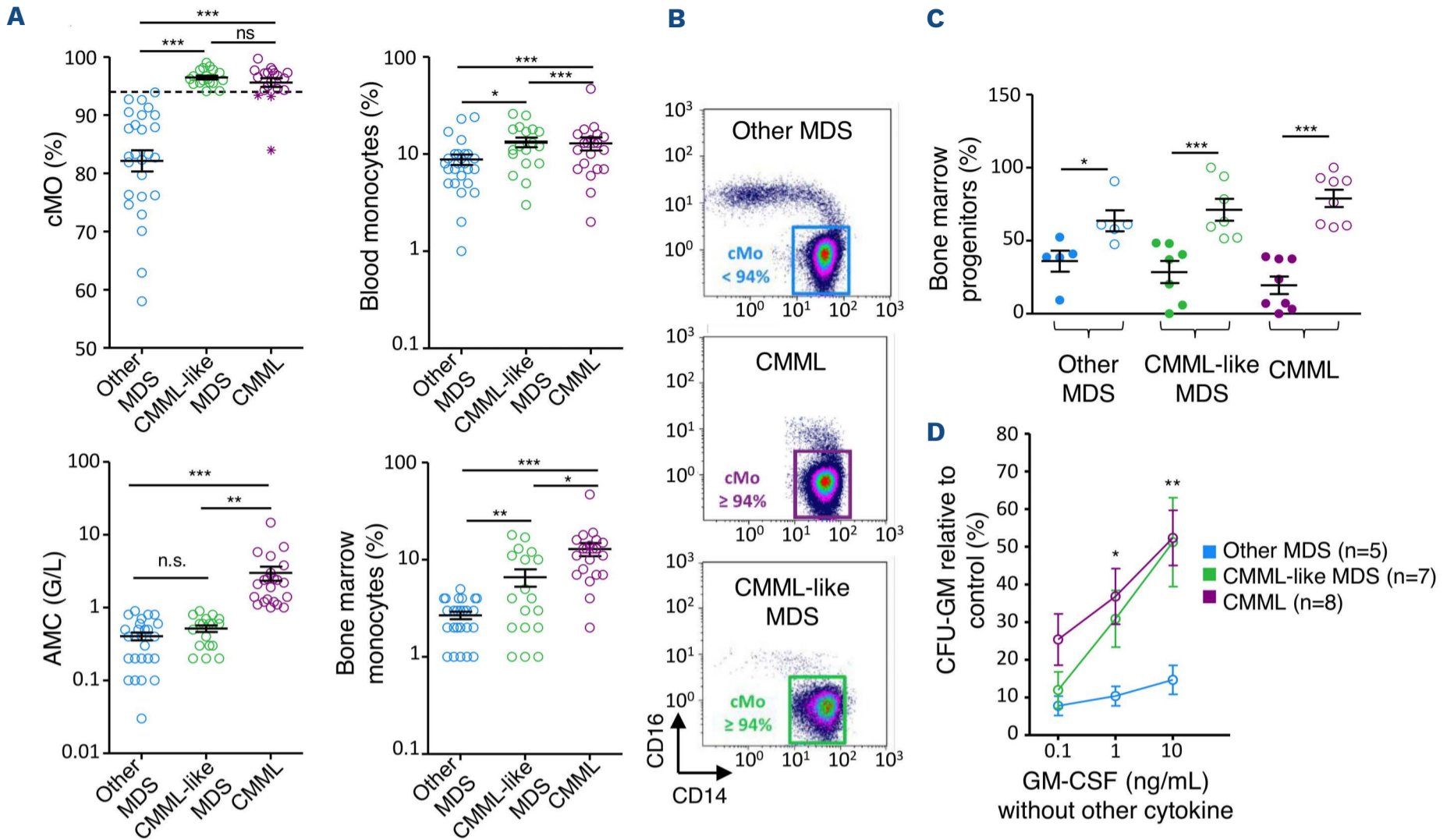
	CMML	MDS			
		Total	CMML-like MDS	Other MDS	P
Patients, N	22	44	18	26	-
Age in years, mean (SD)	68.4 (2.5)	72.0 (1.8)	76.3 (2.5)	69.0 (2.5)	≤ 0.05
Male, N (%)	17 (77.2)	26 (55.3)	12 (66.7)	15 (53.8)	0.2339
Hemoglobin g/dL, mean (SD)	12.2 (0.5)	10.9 (0.3)	10.4 (0.6)	11.3 (0.4)	0.0589
Platelets x10 <sup>9</sup> /L, mean (SD)	167 (22)	178 (19)	178 (35)	177 (23)	0.7353
WBC x10 <sup>9</sup> /L, mean (SD)	10.5 (1.2)	4.7 (0.4)	4.5 (0.6)	4.6 (0.5)	≤ 0.001
ANC x10 <sup>9</sup> /L, mean (SD)	5.4 (0.9)	2.6 (0.3)	2.7 (0.5)	2.7 (0.4)	≤ 0.05
AMC x10 <sup>9</sup> /L, mean (SD)	2.5 (0.4)	0.5 (0.0)	0.5 (0.1)	0.4 (0.1)	≤ 0.001
Blood monocytes %, mean (SD)	24.9 (2.1)	10.6 (0.9)	13.3 (1.5)	8.8 (1.1)	≤ 0.001
Marrow monocytes %, mean (SD)	11 (1)	4 (1)	7 (1)	3 (0.2)	≤ 0.001
Marrow blasts %, mean (SD)	8 (1)	7 (1)	7 (1)	6 (1)	0.0889
Mean MO1 fraction %, (SD)	95.5 (0.7)	88.0 (1.5)	96.9 (0.3)	82.1 (1.7)	≤ 0.001
Patients with cMo ≥94%, N (%)	-	18 (40.9)	-	-	-
<i>De novo</i> diagnosis, N (%)	13 (59.1)	23 (52.3)	11 (61.1)	12 (46.2)	-
IPSS-R (%)	-	39 (88.6)	14 (77.8)	25 (96.2)	0.31
Very low IPSS-R, N (%)	-	5 (12.8)	2 (14.3)	3 (12.0)	-
Low IPSS-R, N (%)	-	18 (46.2)	4 (28.6)	14 (56.0)	-
Intermediate IPSS-R, N (%)	-	10 (25.6)	5 (35.7)	5 (20.0)	-
High IPSS-R, N (%)	-	4 (10.3)	2 (14.3)	2 (8.0)	-
Very high IPSS-R, N (%)	-	2 (5.1)	1 (7.1)	1 (4.0)	-
CPSS, N (%)	21 (95.5)	-	-	-	-
Low CPSS, N (%)	0 (0.0)	-	-	-	-
Intermediate-1 CPSS, N (%)	9 (42.8)	-	-	-	-
Intermediate-2 CPSS, N (%)	6 (28.6)	-	-	-	-
High CPSS, N (%)	6 (28.6)	-	-	-	-

Myelodysplastic syndrome (MDS) patients have been classified into chronic myelomonocytic leukemia (CMML)-like MDS and other MDS according to the presence or absence of classical monocytes (cMO) accumulation ≥94%. Comparisons between CMML, CMML-like and other MDS patients were made using the Kruskal-Wallis test and Chi2 test. SD: standard deviation; WBC: white blood cell count; ANC: absolute neutrophil count; AMC: absolute monocyte count; IPSS-R: revised International Prognostic Scoring System; CPSS: CMML-specific prognostic scoring.

(10/12, 83.3%) compared to other MDS (2/9, 22.2%) patients ( $P=0.0007$  and  $P=0.0092$  respectively, Fisher's exact test) (Figure 2B). The multiple mutations found in CMML and CMML-like MDS patients often showed very similar allelic ratio at around 0.5 and were eventually detected with several additional minor subclones. When CMML-like MDS patients carried a single mutation, the corresponding variant allele frequency (VAF) was above 50% (Figure 2C) indicative of a loss of heterozygosity (LOH). Overall, ten of 12 CMML-like MDS patients carrying *TET2* mutations had,

therefore, mutation VAF indicative of a bi-allelic inactivation of *TET2*, which was observed in only one of nine MDS patients without accumulation of cMO (Figure 1E; Figure 2C; *Online Supplementary Table S2*).

We previously showed that about 50% of MDS patients with cMO accumulation progressed to genuine CMML within 1 year.<sup>1</sup> In the present study, among untreated MDS patients with at least 1 year of follow-up ( $n=21/44$ ), we observed that 55.6% ( $n=5/9$ ) of CMML-like MDS patients progressed to overt CMML (median follow-up 49 months).



Continued on following page.

**Figure 1. A subgroup of myelodysplastic syndromes shares some common features with chronic myelomonocytic leukemia.** (A) Comparison of classical monocyte (cMO) percentage in peripheral blood (PB) (upper left panel) including patients with a bulbous aspect associated to chronic myelomonocytic leukemia (CMML) with an inflammatory state (N=3, purple stars), monocyte percentage in PB (upper right panel), absolute PB monocyte count (AMC) (lower left panel) and monocyte percentage in bone marrow (lower right panel) among “other” myelodysplastic syndromes (MDS) (N=26, blue circles), “CMML-like” MDS (N= 18, green circles) and CMML patients (N=22, purple circles). (B) Examples of monocyte subset repartition in PB analyzed by flow cytometry in “other” MDS with no cMO accumulation (upper panel), while cMO >94% is displayed for CMML (middle panel) and “CMML-like” MDS (lower panel) patients. (C) Comparison of the proportion of erythroid colonies (BFU-E, solid circles) and granulo-monocytic colonies (CFU-GM, empty circles) obtained with colony-forming cell assay (CMML;  $P=0.0009$ ; CMML-like MDS  $P=0.0006$  and in other MDS  $P=0.0159$ , Mann-Whitney test). For each patient,  $10^3$  CD34<sup>+</sup> enriched cells (N=17, CD34 Microbeads Kit, Miltenyi Biotec) or  $7 \times 10^4$  bone marrow mononuclear cells (N=3) were seeded in duplicate in a methylcellulose based-medium with growth factors (Methocult H4434, STEMCELL Technologies) for 14 days at 37°C with 5% CO<sub>2</sub>. Results are expressed as the percentage of all colonies formed by at least 50 cells for “other” MDS (N=5), “CMML-like” MDS (N=7) and CMML (N=8) patients. (D) Colony-forming unit granulocyte-macrophages (CFU-GM) obtained after colony-forming cell assay with the same input cell numbers were seeded in methylcellulose without growth factors (Methocult H4230, STEMCELL Technologies) at various concentrations of granulocyte-macrophage stem cell factor (GM-CSF) (Sandoz; 0 ng/mL, 0.1 ng/mL and 1 ng/mL). Results are expressed as the percentage of CFU-GM found compared to control cultures supplemented with growth factors (50 ng/mL SCF, 10 ng/mL IL-3, 3 U/mL erythropoietin [EPO], and GM-CSF 10 ng/mL, Methocult H4434, STEMCELL Technologies). The upper 95% confidence interval (CI) of the average percentage of normalized colonies derived from “other” MDS patients was calculated for each concentration of GM-CSF tested and used as a cut-off to classify CMML and CMML-like MDS progenitors as hypersensitive. (E) Mutational landscape of CMML, “CMML-like” MDS, and “other” MDS patients included in the learning cohort. Each column represents a patient. Vertical black bars show the total number of mutations detected. Horizontal black bars show the percentage of patients harboring at least one mutation for each gene out of all the patients included in the study. The first line depicts the absence (white square) or the presence of a relative accumulation of cMO  $\geq 94\%$  (green square); an abnormal distribution of monocyte subsets with a bulbous profile associated to CMML with an inflammatory state is represented by a green square with a white asterisk. One patient (represented as a green square with a black asterisk) had an uninterpretable flow cytometry profile due to paroxysmal nocturnal hemoglobinuria. Repartition of monocyte subsets was not available for two patients diagnosed in 2009. Normal karyotype, complex karyotype, and other cytogenetic profiles are shown as light blue square, dark blue square, and blue square, respectively. Revised International Prognostic Scoring System (IPSS-R) score for MDS patients and CMML-specific prognostic scoring (CPSS) score for CMML patients are depicted as low-risk profile (IPSS-R  $\leq 3$  and CPSS  $\leq 1$ , light purple square) or high-risk profile (IPSS-R  $> 3$  and CPSS  $\geq 2$ , dark purple square). In the mutation heatmap, the absence of mutation is shown by a light grey square, one mutation by a yellow square, and multiple mutations by a red square. Multiple mutations are defined by either several gene mutations or a single mutation with a variant allelic frequency (VAF) above 65%. Analysis not performed or uninterpretable results are shown as a dark grey square.

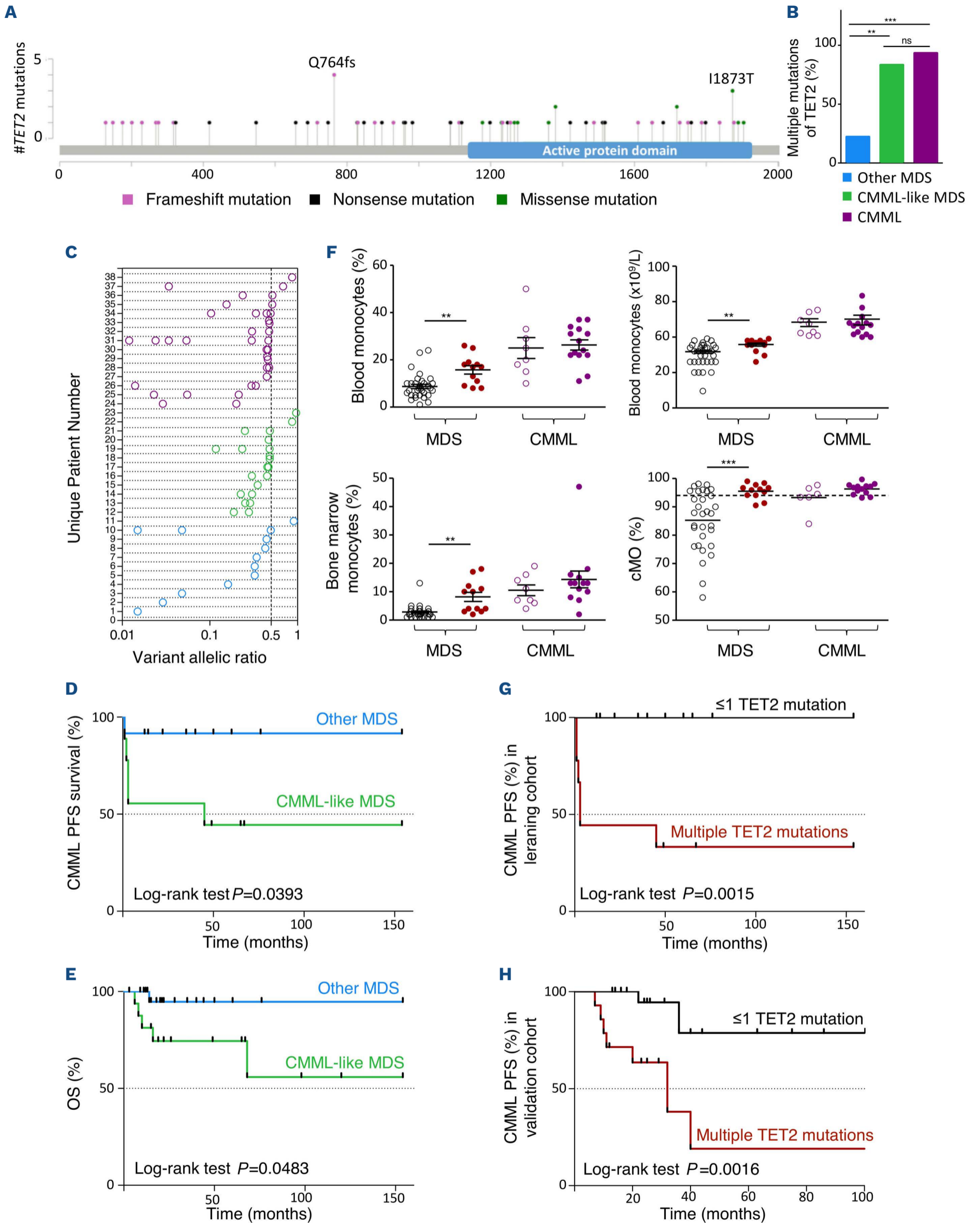
This rate progression to CMML was significantly higher compared with other MDS patients (1/12; 8.3%) ( $P=0.0393$ , log-rank test) (Figure 2D). Of note, CMML-like MDS patients overall survival was significantly reduced compared with other MDS patients ( $P=0.0483$ ; log-rank test) (Figure 2E). This result would need further validation in larger independent cohorts.

We next stratified MDS patients from the learning cohort according to the presence of multiple *TET2* mutations (Figure 2F). MDS patients carrying multiple *TET2* mutations had a significantly increased percentage of peripheral blood ( $15.8 \pm 1.8\%$ ;  $P=0.0025$ , unpaired *t* test with Welch’s correction) and BM ( $8 \pm 2\%$ ;  $P=0.0078$ , unpaired *t* test with Welch’s correction) monocytes compared with other MDS patients. They were significantly older ( $P=0.0269$ , unpaired *t* test with Welch’s correction) and also showed a reduced CMML progression-free survival ( $P=0.0015$ , log-rank test) (Figure 2G) with a median progression-free survival estimated at 3 months. Interestingly, the unique MDS patient without cMO accumulation who progressed to CMML had multiple *TET2* mutations. This result was further confirmed with multicenter validation cohort of 39 untreated MDS patients ( $P=0.0016$ , log-rank test), including 14 patients with multiple *TET2* mutations whose biological features were similar to those

from the learning cohort (Figure 2H; *Online Supplementary Figure S1*; *Online Supplementary Table S1*).

Finally, among all MDS patients analyzed in the learning and validation cohorts, *TET2*<sup>T1873T</sup> (n=4) was significantly associated with evolution to CMML ( $P=0.008$ , LASSO penalized regression).

Recent evolution of myeloid disease classification integrates so-called oligomonocytic CMML,<sup>3</sup> which exhibits characteristic CMML features<sup>4</sup> by decreasing the cut-off value that defines an absolute monocytosis to  $0.5 \times 10^9/L$ .<sup>5</sup> The present study demonstrates that flow cytometry analysis of monocyte subsets in the PB, typically showing an accumulation of cMO  $\geq 94\%$  of total monocytes,<sup>6,7,10</sup> together with typical combinations of somatic gene mutations, detects an additional number of CMML whose initial features are those of an MDS. Their genetic and epigenetic features already point to a CMML, while the characteristic increase in absolute and relative monocyte count will be observed several months or years later.<sup>1</sup> While early identification of an overlap myelodysplastic/myeloproliferative neoplasm (MDS/MPN) may currently have a limited therapeutic impact, these entities deserve to be identified as they may indicate higher risk evolution with decreased survival.<sup>3</sup> In the present study, the MDS to CMML evolution was evaluated in patients that didn’t receive hypomethyl-



Continued on following page.

**Figure 2. *TET2* mutational status and myelodysplastic syndrome evolution to chronic myelomonocytic leukemia.** (A) Lollipop diagram showing mutation distribution across the *TET2* protein in the learning cohort. Sixty-eight mutations from 36 patients are plotted (nonsense mutations are shown in black, frameshift mutations in pink, and missense mutations in green). (B) Patients harboring multiple mutations of *TET2* gene in the 3 subgroups, expressed in percentage among “other” myelodysplastic syndromes (MDS) patients (N=26, blue), “chronic myelomonocytic leukemia (CMML)-like” patients (N=18, green), and CMML patients (N=22, purple). (C) Distribution of variant allelic ratios of *TET2* mutations in the 3 subgroups. Each mutation is shown as a circle for each patient identified by their unique patient number (UPN). The dotted vertical line represents the 50% variant allele frequency (VAF) threshold. (D) Kaplan-Meier CMML progression-free survival (PFS) in “CMML-like” MDS (N=9, green line) and “other” MDS (N=12; blue line). (E) Kaplan-Meier overall survival (OS) in “CMML-like” MDS (N=9; green line) and “other” MDS (N=12; blue line). (F) Monocytes percentage (upper left panel) and AMC (upper right panel) in peripheral blood (PB), monocyte percentage in bone marrow (BM) (lower left panel), and percentage of circulating classical monocyte (cMO) (lower right panel) in the 4 subgroups defined according to their molecular profile: MDS patients carrying multiple *TET2* mutations (solid red circle) or 1 mutation or no *TET2* mutation (open black circle) and CMML patients carrying multiple *TET2* mutations (solid purple circle) or 1 mutation or no *TET2* mutation (open purple circle). (G) Kaplan-Meier CMML PFS of MDS patients carrying multiple *TET2* mutations (N=6, red line) or one mutation or no *TET2* mutation (N=15, black line) in the learning cohort. Multiple mutations are defined by several mutations affecting *TET2* or a unique mutation with a VAF >65%. (H) Kaplan-Meier CMML PFS of MDS patients carrying multiple *TET2* mutations (N=14, red line) or 1 mutation or no *TET2* mutation (N=25, black line) in the validation cohort. In (D, E, G, and H) only patients with a minimal 12-month follow-up were included in the analysis. Patients who received hypomethylating agents after PB monocyte phenotyping were censored.

ating agents or hematopoietic stem cell transplantation. In the future, revisiting the boundaries between MDS and CMML may guide therapeutic approaches targeting the proliferative and highly inflammatory component of CMML to slow down its clinical progression.

As proof of the proliferative component of the disease, CFU-GM hypersensitivity to GM-CSF was observed in both CMML-like MDS and CMML patients and comparable to those previously reported in juvenile myelomonocytic leukemia and CMML.<sup>8</sup> Myeloid colony formation becomes independent of growth factors in a subset of highly proliferative CMML patients, which commonly correlates with clonal evolution including the acquisition of RAS pathway mutations,<sup>11</sup> and is associated with an inferior outcome.<sup>12</sup> In the present study, GM-CSF hypersensitivity was identified in patients who didn't carry signaling mutations. The NGS panel covered most of the recurrently mutated signaling genes described in myeloid malignancies except *NF1*. Interestingly, a previous study showed efficient inhibition of CMML cell growth using an anti-GM-CSF antibody regardless of signaling gene mutations.<sup>8</sup>

Clonal architecture analysis showed that *TET2* mutation is often the first hit in CMML,<sup>13</sup> and bi-allelic *TET2* inactivation may be a key event in driving the disease phenotype, either oligo-CMML or the full-blown disease.<sup>3,14</sup> We noticed that the most frequent *TET2* missense mutation *TET2*<sup>I1873T</sup>, was associated with bi-allelic alteration of *TET2* and identified as a significantly independent factor of CMML evolution. *TET2*<sup>I1873T</sup> is located in a conserved region of the DSBH domain, and its functional impact is still only partially understood.

In conclusion, a combination of phenotypic, genomic and functional features defines a subset of MDS patients who may eventually evolve into CMML, revisiting the boundaries between MDS and MDS/MPN and potentially defining a subgroup of patients with a poorest outcome.<sup>3</sup> It may guide future therapeutic strategies targeting the prolifer-

ative and highly inflammatory component of CMML to slow down its clinical progression, such as lenzilumab, an anti-GM-CSF monoclonal antibody. These results also point to the usefulness of combining flow cytometry of peripheral blood monocyte subsets and analysis of their mutational status to better classify patients with dysplastic features.<sup>15</sup>

## Authors

Violaine Tran Quang,<sup>1,2</sup> Benjamin Podvin,<sup>3\*</sup> Christophe Desterke,<sup>4\*</sup> Sihem Tarfi,<sup>1,2</sup> Quentin Barathon,<sup>2</sup> Bouchra Badaoui,<sup>2</sup> Nicolas Freynet,<sup>2</sup> Vincent Parinet,<sup>1,5</sup> Mathieu Leclerc,<sup>1,5</sup> Sébastien Maury,<sup>1,5</sup> Eric Solary,<sup>6</sup> Dorothée Selimoglu-Buet,<sup>6</sup> Nicolas Duployez,<sup>4</sup> Oriane Wagner-Ballon<sup>1,2#</sup> and Ivan Sloma<sup>1,2#</sup>

<sup>1</sup>Université Paris Est Créteil, INSERM, IMRB, Créteil; <sup>2</sup>AP-HP, Hôpital Henri Mondor, Département d'Hématologie et Immunologie, Créteil;

<sup>3</sup>Centre Hospitalier Régional Universitaire de Lille, Laboratoire d'Hématologie, Lille; <sup>4</sup>Université Paris-Sud, Faculté de Médecine Kremlin Bicêtre, INSERM UMS 33, Villejuif; <sup>5</sup>AP-HP, Hôpital Henri Mondor, Département d'Hématologie, Créteil and <sup>6</sup>INSERM Unité Mixte de Recherche (UMR) 1287, Faculté de Médecine, Université Paris-Sud, Gustave Roussy, Villejuif, France

\*BP and CD contributed equally.

#OW-B and IS contributed equally as senior authors.

Correspondence:

I. SLOMA - ivan.sloma@aphp.fr

<https://doi.org/10.3324/haematol.2022.282528>

Received: January 11, 2023.

Accepted: April 14, 2023.

Early view: April 27, 2023.

©2023 Ferrata Storti Foundation

Published under a CC BY-NC license 

**Disclosures**

ES, DS-B, and OW-B have a patent issued relevant to the work. The remaining authors have no conflicts of interest to disclose.

**Contributions**

VTQ performed flow cytometry and cellular bone marrow analyses, progenitor assays, and helped to write the manuscript. CD performed the LASSO biostatistics analysis. ST, BB and NF also performed flow cytometry analyses. QB prepared the NGS library with help from VTQ. SM, VP and ML provided patient samples. BP

and ND provided biological and clinical data. ES and DS-B critically reviewed the article. IS developed and validated the NGS panel design, the bioinformatics pipeline and performed tertiary NGS analysis with help from VTQ. OW-B and IS designed the study and wrote the manuscript.

**Acknowledgments**

We thank Alban Lermine and the Bioinformatics platform MOABI from Assistance Publique-Hôpitaux de Paris for bioinformatics pipeline implementation in routine clinical practice. VTQ received a fellowship from la Fondation pour la Recherche Médicale.

**Data-sharing statement**

The supporting data are available in the *Online Supplementary Table S2*.

## References

---

1. Selimoglu-Buet D, Badaoui B, Benayoun E, et al. Accumulation of classical monocytes defines a subgroup of MDS that frequently evolves into CMML. *Blood*. 2017;130(6):832-835.
2. Kasprzak A, Assadi C, Nachtkamp K, et al. Monocytosis at the time of diagnosis has a negative prognostic impact in myelodysplastic syndromes with less than 5% bone marrow blasts. *Ann Hematol*. 2023;102(1):99-106.
3. Calvo X, Garcia-Gisbert N, Parraga I, et al. Oligomonocytic and overt chronic myelomonocytic leukemia show similar clinical, genomic, and immunophenotypic features. *Blood Adv*. 2020;4(20):5285-5296.
4. Garcia-Gisbert N, Arenillas L, Roman-Bravo D, et al. Multi-hit TET2 mutations as a differential molecular signature of oligomonocytic and overt chronic myelomonocytic leukemia. *Leukemia*. 2022;36(12):2922-2926.
5. Khoury JD, Solary E, Abla O, et al. The 5th edition of the World Health Organization classification of haematolymphoid tumours: myeloid and histiocytic/dendritic neoplasms. *Leukemia*. 2022;36(7):1703-1719.
6. Talati C, Zhang L, Shaheen G, et al. Monocyte subset analysis accurately distinguishes CMML from MDS and is associated with a favorable MDS prognosis. *Blood*. 2017;129(13):1881-1883.
7. Selimoglu-Buet D, Wagner-Ballon O, Saada V, et al. Characteristic repartition of monocyte subsets as a diagnostic signature of chronic myelomonocytic leukemia. *Blood*. 2015;125(23):3618.
8. Padron E, Painter JS, Kunigal S, et al. GM-CSF-dependent pSTAT5 sensitivity is a feature with therapeutic potential in chronic myelomonocytic leukemia. *Blood*. 2013;121(25):5068-5077.
9. Gricourt G, Tran Quang V, Cayuela J-M, et al. Fusion gene detection and quantification by asymmetric capture sequencing (aCAP-Seq). *J Mol Diagn*. 2022;24(11):1113-1127.
10. Patnaik MM, Timm MM, Vallapureddy R, et al. Flow cytometry based monocyte subset analysis accurately distinguishes chronic myelomonocytic leukemia from myeloproliferative neoplasms with associated monocytosis. *Blood Cancer J*. 2017;7(7):e584-e584.
11. Geissler K, Jäger E, Barna A, et al. Chronic myelomonocytic leukemia patients with RAS pathway mutations show high in vitro myeloid colony formation in the absence of exogenous growth factors. *Leukemia*. 2016;30(11):2280-2281.
12. Geissler K, Jäger E, Barna A, et al. Correlation of RAS-pathway mutations and spontaneous myeloid colony growth with progression and transformation in chronic myelomonocytic leukemia - a retrospective analysis in 337 patients. *Int J Mol Sci*. 2020;21(8):3025.
13. Itzykson R, Kosmider O, Renneville A, et al. Clonal architecture of chronic myelomonocytic leukemias. *Blood*. 2013;121(12):2186-2198.
14. Awada H, Nagata Y, Goyal A, et al. Invariant phenotype and molecular association of biallelic TET2 mutant myeloid neoplasia. *Blood Adv*. 2019;3(3):339-349.
15. Solary E, Wagner-Ballon O, Selimoglu-Buet D. Incorporating flow cytometry and next-generation sequencing in the diagnosis of CMML. Are we ready for prime? *Best Pract Res Clin Haematol*. 2020;33(2):101134.